LETTERS

Boundary lubrication under water

Wuge H. Briscoe[1], Simon Titmuss[1], Fredrik Tiberg[1]†, Robert K. Thomas[1], Duncan J. McGillivray[1]† & Jacob Klein[1,2]

Boundary lubrication, in which the rubbing surfaces are coated with molecular monolayers, has been studied extensively for over half a century[1–7]. Such monolayers generally consist of amphiphilic surfactants anchored by their polar headgroups; sliding occurs at the interface between the layers, greatly reducing friction and especially wear of the underlying substrates. This process, widespread in engineering applications, is also predicted to occur in biological lubrication via phospholipid films[8,9], though few systematic studies on friction between surfactant layers in aqueous environments have been carried out[5,10]. Here we show that the frictional stress between two sliding surfaces bearing surfactant monolayers may decrease, when immersed in water, to as little as one per cent or less of its value in air (or oil). We attribute this to the shift of the slip plane from between the surfactant layers, to the surfactant/substrate interface. The low friction would then be due to the fluid hydration layers surrounding the polar head groups attached to the substrate. These results may have implications for future technological and biomedical applications.

Normal and shear forces $F_\perp$ and F_s respectively are measured between two atomically smooth curved mica surfaces (radius of curvature $R \approx 1$ cm) using a surface force balance described previously[11]. This is carried out first in dry air (in the presence of P_2O_5), then when bearing the double-chained cationic surfactant DDunAB[12], *N*,*N*-dimethyl-*N*,*N*-diundecylammonium bromide with structure $(CH_3(CH_2)_{10})_2N^+(CH_3)_2Br^-$, typical of a large class of similar amphiphilic surfactants, both in dry air and in (surfactant-free) water. We carried out some ten separate experiments on the DDunAB with surfactant layers formed by incubation times ranging from 10 min to 120 min.

Normalized force $F_\perp$ versus separation D profiles, $F_\perp(D)/R$, including controls between surfaces of bare mica before surfactant self-assembly, are shown in Fig. 1. The surfactant-coated surfaces experience the expected strong adhesion both in dry air and in water[13,14]. The total surfactant layer thickness in dry air contact is $D_0 = 2.7 \pm 0.4$ nm, smaller than twice the total extended molecular length of the surfactant, 3.8 nm, indicating that the molecules adsorb onto each mica surface with the hydrocarbon tails tilted. On adding water the layers swelled slightly, as revealed by an increase of the contact separation after the first approach and adhesion in water (averaged over all experiments), by an amount $\Delta D_0 = 0.51 \pm 0.4$ nm. The magnified-scale inset in Fig. 1 reveals the long-range attraction from $D \approx 30$ nm, before the jump into contact characteristic of hydrophobic interactions[14]. The strong adhesion that the surfaces experience in contact (in both air and water), deforms them elastically[15] to form a flattened, roughly circular contact zone between them with an area A (see interference fringes in Fig. 2) of the order of 1,000 μm^2. It is across this flattened, strongly adhering region that we measure the friction force F_s between the surfaces.

The frictional response between the surfactant-coated surfaces as the top surface moves laterally back-and-forth after a first approach is shown in Fig. 2. In dry air (trace B in Fig. 2) the surfaces remain rigidly coupled to each other for all applied shear amplitudes Δx_0 (10–1,800 nm). The friction force F_s between the surfaces must thus exceed the maximum applied shear force ($F_s > F_{max} = 200$–250 μN), corresponding to a sliding shear stress between the surfaces, $\sigma_s = F_s/A > 0.2$ MPa. This is consistent with the range of previous

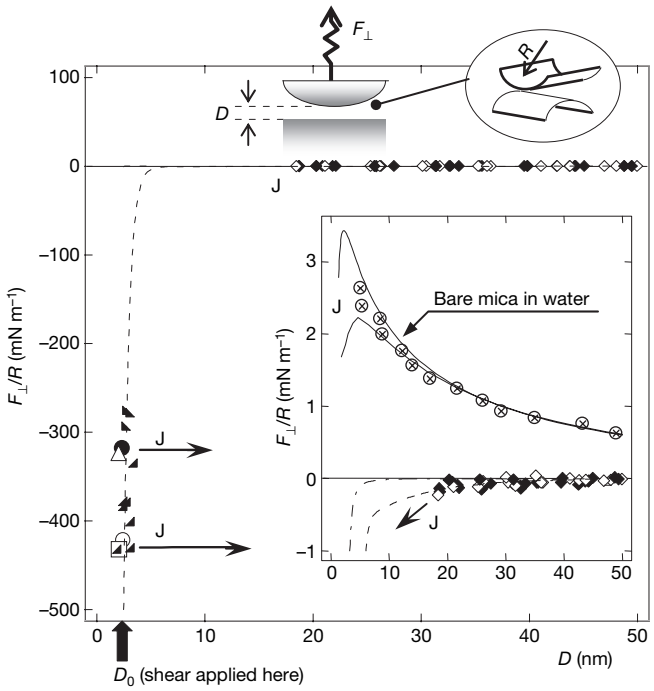

Figure 1 | Normal interactions $F_\perp/R$ between DDunAB-coated crossed-cylindrical mica surfaces (radius of curvature R is ~1 cm), as a function of closest separation D. Forces $F_\perp$ were measured with a surface force balance[11] (cartoon). Different symbols indicate separate experiments (10-min or 120-min layers, see Methods). The open triangle and closed circle represent adhesive contact in dry air (mean of several measurements). The closed and open diamonds represent interaction profiles across water with no added salt, up to jumps (J) into adhesive contact. The open square and circle indicate adhesive contact following first approach in water. The adhesion in water on subsequent approaches following shear is similar or slightly decreased (◢ is 120 min, and ◣ is 10 min). The inset shows interactions on an enlarged scale: crossed circles represent interactions between the bare mica surfaces (solid curves show expected DLVO double-layer forces[13]. Upper solid curve, constant surface charge density of 0.0048 C m^{-2}; lower solid curve, constant surface potential of 155 mV; both with 1.5×10^{-5} M 1:1 background electrolyte concentration). Other symbols as in the main figure. The lowest curves are van der Waals attraction (dot-dashed curve) and an empirical double exponential function (dashed curve) characteristic of hydrophobic attraction[14]. All measurements are at 25 ± 0.5 °C.

[1]Physical and Theoretical Chemistry Laboratory, University of Oxford, South Parks Road, Oxford OX1 3QZ, UK. [2]Weizmann Institute of Science, Rehovot 76100, Israel. †Present addresses: Camrus AB, Ideon Science Park, Sölvegatan 41, SE-223 70 Lund, Sweden (F.T.); Department of Biophysics, Johns Hopkins University, Baltimore, Maryland 21218, USA (D.J.M.).

studies[2,10,16] of the frictional shear stress between surfactant-coated surfaces in dry air at comparable normal stresses and velocities. Once water is introduced between the surfactant-coated surfaces, the sliding frictional stress between them when in adhesive contact is strikingly reduced relative to air, despite the stronger adhesion under water (Fig. 1). A typical friction trace C following initial contact is shown in Fig. 2.

Figure 3 summarizes the measured sliding friction stresses $\sigma_s = F_s/A$ between the surfactant layers under water at different shear velocities v_s, revealing a weak velocity dependence in line with earlier studies[2,6,10]. The shaded part of the inset to Fig. 3 shows the range of frictional stresses taken from earlier studies[2,3,10,16], covering a wide spectrum of boundary surfactants and conditions in air. The most remarkable feature of our data is the very substantial reduction—by up to 99% or more—of σ_s under water relative to its value in air.

What is the origin of this very large decrease in the friction when the sliding occurs under water? In the case of friction between similar surfactant layers in air, a coherent picture has emerged (for example, see refs 3 and 17), correlating the frictional stress σ_s during sliding with the loading/unloading adhesion hysteresis $\Delta\gamma$ between the boundary layers. The relation $\Delta\gamma/\delta \cong \sigma_s$, where δ is a microscopic length scale (of the order of 1 nm or less), accounts well for the frictional dissipation in a wide range of conditions (in air) as the surfactant-coated surfaces slide past each other[3]. However, we attribute the striking reduction in friction under water relative to dry air observed here to a conceptually quite different origin. It is due, we believe, to the shift of the slip plane from between the boundary lubricant layers to the surfactant–substrate interface.

This occurs because of the facile penetration of water and consequent hydration of the anchoring polar headgroups at the solid substrate[3,17,18], consistent with the known high mobility of water in comparable surfactant layers[19,20]. It is significant in this context that the swelling $\Delta D_0/2$ of each monolayer on adding water (0.26 ± 0.2 nm) is close to the swelling due specifically to hydration of headgroups (0.25 nm), measured[18] for similar confined surfactant monolayers on going from the dry state to immersion in water. The resulting hydration sheaths efficiently lubricate the lateral motion of the headgroups on the surface, in strong analogy with the recently observed lubrication provided by hydrated metal ions between solid surfaces[21,22]. As a result, the interface with least resistance to shear becomes that between the surfactant headgroups and the substrate, rather than the surfactant–surfactant interface (where sliding classically occurs in air or oil). It is therefore to that weaker interface that the slip plane reverts as the surfaces slide past each other.

To test this hypothesis—which contrasts with the accepted mechanism for boundary lubrication in air or oil—more directly, we carried out the following three experiments. First, we determined the adhesion hysteresis $\Delta\gamma$ between the surfactant layers both in dry air and under water, by monitoring the contact area during loading/unloading cycles (Methods section). The results, shown in Fig. 4, reveal that the magnitude of $\Delta\gamma$ is in the range (20 ± 2) mJ m^{-2} both in air and under water. Putting $\Delta\gamma/\delta \cong \sigma_s$, with $\delta = 1$ nm, yields a

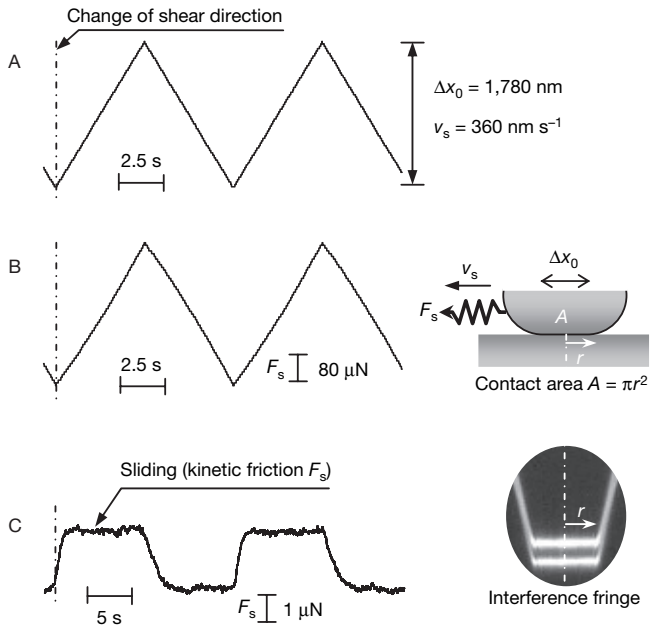

Figure 2 | Characteristics of measured friction between two DDunAB-coated surfaces in adhesive contact. Trace A, back-and-forth shear amplitude Δx_0 applied with time to the top surface; traces B and C, the corresponding shear force F_s transmitted across the surfactant layers. Trace B, dry air, showing rigid coupling of the surfaces, that is, the frictional force exceeds the shear force up to the maximal applied shear amplitude. Trace C is a typical transmitted shear force versus time trace between the two surfactant layers (10 min) in adhesive contact after addition of pure water. The lower right-hand insets illustrate the surface force balance configuration in shear[11] and the region over which friction was measured from the corresponding fringe image taken from an actual experiment.

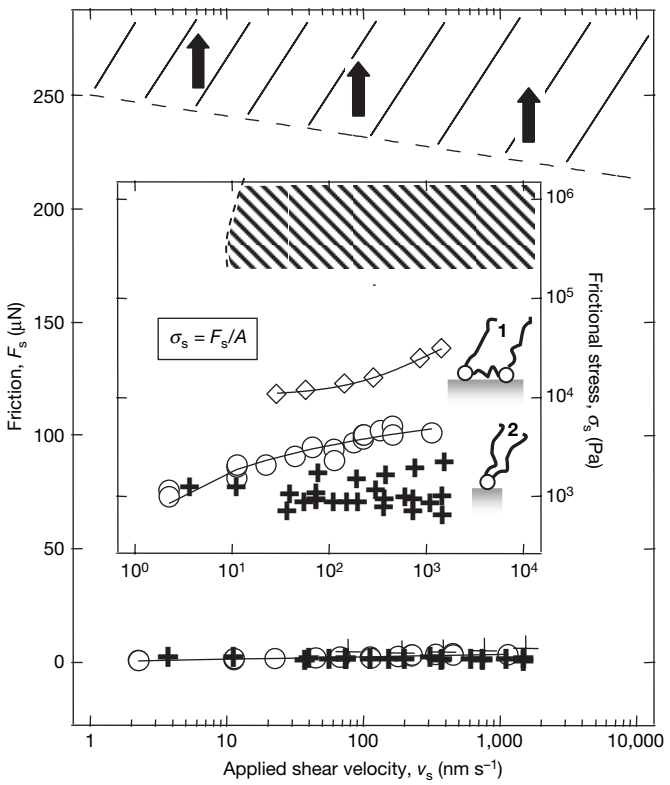

Figure 3 | Dependence of friction force F_s between surfactant layers in initial contact in water on the sliding velocity v_s. F_s is measured from traces such as B and C in Fig. 2. The friction forces in dry air (before adding water) at all velocities and for all surfactants are greater than the upper hatched region. Open circles indicate DDunAB layers (10 min), measured following approach to adhesion across water. Crosses indicate DDunAB layers (10 min) that were in adhesive contact before immersion in water and throughout the friction measurements. The inset shows the corresponding frictional sliding stress $\sigma_s = F_s/A$, where the contact area A between the two surfaces is measured from the flat portion of the optical fringes (as inset in Fig. 2). The data symbols in the inset for DDunAB (schematic **2**) correspond to those in the main figure. (The data are identical in the inset and the main figure: the logarithmic scale of the inset highlights the variation of the data relative to that of the linear scale of the main figure.) Open diamonds in the inset indicate frictional sliding stress for the Gemini surfactant (see text; schematic **1**). The dry air contact separation between the Gemini-monolayer-bearing surfaces is 1.3 ± 0.3 nm. The hatched area shows, for comparison, the range of frictional sliding stresses from several other comparable experiments[2,3,10,16] in air (dry, humid or with organic vapour). The solid curves are a guide to the eye.

frictional sliding stress $\sigma_s \approx 2 \times 10^7$ N m^{-2}, which is within the range of the frictional stress regime in dry air, but is too high, by some orders of magnitude, to account for the low friction under water, for which $\sigma_s = (1–5) \times 10^3$ N m^{-2} (inset to Fig. 3). The clear implication is that while, in air, both adhesion and sliding occur at the same surfactant–surfactant interface, the situation under water is different: The weakest adhesion (and therefore separation of the surfaces on pull-off) occurs at the surfactant–surfactant interface, but the sliding under water must occur at a much more lubricated interface: the one between the surfactant headgroups and the substrate. This unexpected result is, however, consistent with estimates of the magnitude of the adhesion at the two interfaces (Methods).

Second, to eliminate the possibility that the sliding may nonetheless have been occurring at the mid-plane, lubricated by hydrated polar headgroups of surfactant molecules that had undergone an overturning or 'flip-flop' transition[23,24] under water, we repeated the frictional experiments using a different procedure. Following measurements in dry air, the surfaces were brought into adhesive contact at $D = D_0 = 2.7 \pm 0.4$ nm as before. On subsequent addition of water, the contact separation increased by 0.6 ± 0.4 nm, very similar to the swelling $\Delta D_0 = 0.51 \pm 0.4$ nm noted earlier for monolayers which were immersed in water before contact. Frictional forces were then measured as above, taking care not to separate the contacting regions or expose them directly to water at any time during the shear. The frictional stresses measured in this way are shown as the crosses (data points) in Fig. 3. They reveal a comparable (or even slightly lower) frictional stress than when water is introduced before contact. With this procedure the possibility of any overturning of surfactants[23,24] and consequent hydration of the surfactant–surfactant interface is suppressed, so we conclude that the slip-plane must indeed be at the surfactant-substrate interface.

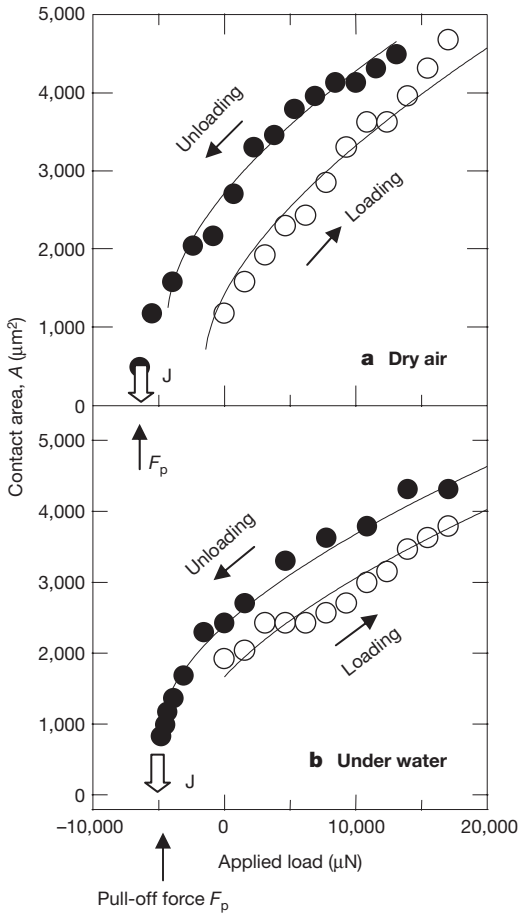

Figure 4 | Loading–unloading profiles of contacting DDunAB (10 min) layers showing variation of contact area *A* with load *L*. **a**, In dry air; **b**, under water. The solid lines are fits to the Johnson-Kendall-Roberts expression (see Methods) using best-fit values of the adhesion energy γ on loading (γ_L) and unloading (γ_U), and yield differences $\Delta\gamma = (\gamma_U - \gamma_L)$ in the range 20 ± 2 mJ m^{-2} for both cases (differences in absolute pull-off forces are due to different unperturbed radii of curvature *R*).

Finally, we measured the friction using a boundary lubricant of chemical structure homologous to DDunAB above, but with different architecture, so that it contacts the surface not only via its polar headgroups but also via hydrophobic moieties. We used the symmetric Gemini surfactant $CH_3(CH_2)_{11}$–$N^+(CH_3)_2Br^-$–$(CH_2)_6$–$N^+(CH_3)_2Br^-$–$(CH_2)_{11}CH_3$, which contacts the mica via its two polar ($N^+(CH_3)_2$) headgroups, as well as via the intervening $(CH_2)_6$ spacer, as revealed by neutron reflectometery and indicated by schematic **1** in the inset to Fig. 3 (R.K.T. and P. X. Li, unpublished data; see also Supplementary Information). Typical sliding frictional stresses using these surfactants immersed in water are summarized in the inset to Fig. 3. They are lower than for boundary lubrication in air, but are higher than for the DDunAB molecules. This is in line with our expectation that only the polar headgroups of the surfactant layers can become hydrated and provide lubrication. The DDunAB layers have a relatively more hydrated interface with the substrate (schematic **2** in the inset to Fig. 3), and therefore slide more easily than the other surfactant, for which only part of the surfactant/substrate interface is hydrated, the rest being covered by the hydrophobic C_6 alkyl groups—which cannot be hydrated—in close proximity to the surface.

In summary, we have shown that the frictional stress between sliding surfaces coated with amphiphilic surfactant layers (boundary lubricants) immersed in water may be reduced by 1–2 orders of magnitude or more, relative to its value in dry air. We attribute this to the shift of the slip plane during frictional sliding, from the surfactant–surfactant midplane interface (in air) to the much better lubricated surfactant–substrate interfaces (under water). Lubrication at the latter interfaces is mediated, we believe, by the fluid hydration sheaths surrounding the surfactant polar headgroups at the substrate, in analogy to the lubricating effect provided by hydrated ions between compressed sliding surfaces[21]. This unexpected scenario of crossover of the slip plane is supported by several observations: pre-adhering the surfaces before their immersion in water results in similarly low friction, indicating that fluidization of the surfactant–surfactant interface cannot be responsible for the lubrication. In addition, the large adhesion hysteresis both in air and in water indicates adhesion occurs at a different interface (between the surfactants) to that of sliding (at the substrate–surfactant interface). Finally, using chemically homologous surfactants of different architecture can result in much higher friction, as expected when the surfactant–substrate interface is only partly hydrated.

Our results may have implications for the lubrication of biomedical devices and microelectromechanical systems currently limited by friction and wear: for example, in the design of boundary lubricant molecules that will optimize the extent of interfacial hydration. The results suggest applications in living systems that are in aqueous environments: their lubrication may also be mediated by hydration shells (in contrast to conjectures that a classical boundary lubrication mechanism is active[8]), and may point to more efficient treatments for osteoarthritis[25].

METHODS

Boundary layer preparation. After calibrating in air contact, the mica surfaces glued onto cylindrical silica lenses (Epon 1004, Shell) were dismounted and immersed for different periods from 10–120 min in the surfactant solution, 0.3–3 mM concentration (~10–100-fold critical micelle concentration) at ~25 °C in water (purified via the RiOs5-MilliQ Gradient A10 system; resistivity is >18.2 Ω cm and total organic content ≤4 p.p.b.). In the figure legends, layers prepared at these different incubation times are identified as '10 min' and so on. After withdrawal from the surfactant solution, the surfaces were rinsed thoroughly with water, and dried in a desiccator in the presence of P_2O_5 for ~15 h before being remounted in the surface force balance (in the presence of P_2O_5).

The double surfactant layer thickness is 2.2 ± 0.3 nm relative to air, to which 5 ± 3 Å was added to account for the thin adsorbed water/gas layer known to desorb in water[21], which presumably comes off on immersion in the surfactant solution.

Adhesion hysteresis. The contact area A between the surfaces is varied (and monitored) by changing the load L during compression or decompression runs to yield the data in Fig. 4, from which the adhesion energy γ may be extracted by fitting the $A(L)$ variation to the Johnson-Kendall-Roberts contact mechanics expression[15]:

$$A = \pi\{(R/K)[L + 6\pi R\gamma + (12\pi R\gamma L + (6\pi R\gamma)^2)^{1/2}]\}^{2/3} \qquad (0)$$

Here $K = 9.5 \times 10^9$ N m^{-2} is the effective modulus of the mica/glue combination. The difference between the value of γ on loading (γ_L) and its value on unloading (γ_U) gives the adhesion energy hysteresis $\Delta\gamma$.

Adhesive forces at the different interfaces. We assume the monolayers detach intact on pull-off so that surfactant molecules remain within their layers. The hydrophobic adhesive force $f_{surf-surf}$ per surfactant molecule at the surfactant–surfactant interface may be written as[14] $f_{surf-surf} = [\partial E/\partial D]_{D=0}$ where $E \approx (\gamma s^2)e^{-D/h}$; here $\gamma \approx 35$ mJ m^{-2} is the surface energy at the interface between the hydrophobic tail and the water (from the pull-off forces in Fig. 1), $s^2 \approx 50$ Å^2 is the mean area per surfactant molecule, and $h \approx 1$ nm is the decay length for the hydrophobic attraction[14]. This yields $f_{surf-surf} = (\gamma s^2)/h \approx 2 \times 10^{-11}$ N. The adhesive force $f_{surf-substr}$ per surfactant molecule attached by a positively charged polar head at the negatively charged substrate may be estimated as $f_{surf-substr} = -e^2/(4\pi\varepsilon\varepsilon_0 x^2)$, where $x \approx 4$ Å is the charge separation and e is the electronic charge. The effective dielectric constant for layers of water comparable in thickness l to a hydration layer is much less than that of the bulk, and has been both calculated[26] and evaluated from experiment[27] as $\varepsilon \approx 5$–10 for $l < 1$ nm. This gives $f_{surf-substr} \approx (1–2) \times 10^{-10}$ N, an order of magnitude or so larger than $f_{surf-surf}$ (this estimate assumes the hydration layers detach with the polar headgroups, to be replaced by water at the mica surface). This is consistent with pull-off on separation of the surfaces occurring at the surfactant–surfactant interface, even though sliding occurs at the substrate surfaces.

Received 10 May; accepted 24 August 2006.

1. Bowden, F. P. & Tabor, D. D. *The Friction and Lubrication of Solids* Vols I and II (Oxford Univ. Press, Oxford, 1950, 1964).
2. Briscoe, B. J. & Evans, D. C. B. The shear properties of Langmuir-Blodgett layers. *Proc. R. Soc. Lond. A* **380,** 389–407 (1982).
3. Yoshizawa, H., Chen, Y-L. & Israelachvili, J. Fundamental mechanisms of interfacial friction. 1. Relation between adhesion and friction. *J. Phys. Chem.* **97,** 4128–4140 (1993).
4. Zhang, L., Li, L., Chen, S. & Jiang, S. Measurements of friction and adhesion for alkyl monolayers on Si(111) by scanning force microscopy. *Langmuir* **18,** 5448–5456 (2002).
5. Grant, L. M. & Tiberg, F. Normal and lateral forces between lipid covered solids in solutions: correlation between layer packing and structure. *Biophys. J.* **82,** 1373–1385 (2002).
6. Suda, H. Origin of friction derived from rupture dynamics. *Langmuir* **17,** 6045–6047 (2001).
7. Zilberman, S., Persson, B. N. J. & Nitzan, A. Theory and simulations of squeeze-out dynamics in boundary lubrication. *J. Chem. Phys.* **115,** 11268–11277 (2001).
8. Hills, B. A. Boundary lubrication *in vivo*. *Proc. Inst. Mech. Eng. H* **214,** 83–94 (2000).
9. Sarma, A. V., Powell, G. L. & LaBerge, M. Phospholipid composition of articular cartilage boundary lubricant. *J. Orthop. Res.* **19,** 671–676 (2001).
10. Drummond, C., Israelachvili, J. & Richetti, P. Friction between two weakly adhering boundary lubricated surfaces in water. *Phys. Rev. E* **67,** 066110 (2003).
11. Klein, J. & Kumacheva, E. Simple liquids confined to molecularly thin layers. I. Confinement-induced liquid to solid phase transitions. *J. Chem. Phys.* **108,** 6996–7009 (1998).
12. McGillivray, D. J., Thomas, R. K., Rennie, A. R., Penfold, J. & Sivia, D. S. Ordered structures observed at the silicon-water interface for di-chain cationic surfactants. *Langmuir* **19,** 7719–7726 (2003).
13. Derjaguin, B. V., Churaev, N. V. & Muller, V. M. *Surface Forces* Ch. 4 and 8 (Consultants Bureau, New York, 1987).
14. Christenson, H. K. & Claesson, P. M. Direct measurements of the forces between hydrophobic surfaces in water. *Adv. Colloid Interf. Sci.* **91,** 391–436 (2001).
15. Johnson, K. L., Kendall, K. & Roberts, A. D. Surface Mechanics and the contact of elastic solids. *Proc. R. Soc. Lond. A* **324,** 301–313 (1971).
16. Yamada, S. & Israelachvili, J. N. Friction and adhesion hysteresis of fluorocarbon surfactant monolayer-coated surfaces measured with the surface forces apparatus. *J. Phys. Chem. B* **102,** 234–244 (1998).
17. Chen, Y. L. & Israelachvili, J. N. Effects of ambient conditions on adsorbed surfactant and polymer monolayers. *J. Phys. Chem.* **96,** 7752–7760 (1992).
18. Williams-Daryn, S., Thomas, R. K., Castro, M. A. & Becerro, A. Structure of complexes of Vermiculite intercalated by cationic surfactants. *J. Colloid Interf. Sci.* **256,** 314–324 (2002).
19. Wennerstrom, H., Persson, N. O. & Lindman, B. in *Colloidal Dispersions and Micellar Behaviour* (ed. Mittal, K. L.) Ch. 18 253–269 (ACS Symp. Ser. 9, American Chemical Society, Washington, 1975).
20. Hamnerius, Y., Lundström, I., Paulsson, L. E., Fontell, K. & Wennerström, H. Dielectric properties of lamellar lipid water phases. *Chem. Phys. Lipids* **22,** 135–140 (1978).
21. Raviv, U. & Klein, J. Fluidity of bound hydration layers. *Science* **297,** 1540–1543 (2002).
22. Raviv, U., Giasson, S., Gohy, J-F., Jerome, R. & Klein, J. Lubrication by charged polymers. *Nature* **425,** 163–165 (2003).
23. Chen, Y. L. E., Gee, M. L., Helm, C. A., Israelachvili, J. N. & McGuiggan, P. M. Effects of humidity on the structure and adhesion of amphiphilic monolayers on mica. *J. Phys. Chem.* **93,** 7057–7059 (1989).
24. Langmuir, I. Overturning and anchoring of monolayers. *Science* **87,** 493–500 (1938).
25. Vecchio, P., Thomas, K. & Hills, B. A. Surfactant treatment for osteoarthritis. *Rheumatology* **38,** 1020–1021 (1999).
26. Stern, H. A. & Feller, S. E. Calculation of the dielectric permittivity profile for a nonuniform system. *J. Chem. Phys.* **118,** 3401–3412 (2003).
27. Teschke, O., Ceotto, G. & de Souza, E. F. Dielectric exchange force: a convenient technique for measuring the interfacial water relative permittivity profile. *Phys. Chem. Chem. Phys.* **3,** 3761–3768 (2001).

Supplementary Information is linked to the online version of the paper at www.nature.com/nature.

Acknowledgements We thank M. Chen and P.X. Li for experimental assistance, and I. Dunlop, J. Israelachvili, S. Perkin and B. Roux for comments. Financial support from the EPSRC (UK) and from the Israel Science Foundation (J.K.) is acknowledged with thanks.

Author Information Reprints and permissions information is available at www.nature.com/reprints. The authors declare no competing financial interests. Correspondence and requests for materials should be addressed to J.K. (jacob.klein@chem.ox.ac.uk or jacob.klein@weizmann.ac.il).